

EigenTrack: Spectral Activation Feature Tracking for Hallucination and Out-of-Distribution Detection in LLMs and VLMs

Davide Ettori¹, Nastaran Darabi¹, Sina Tayebati¹, Ranganath Krishnan², Mahesh Subedar³, Omesh Tickoo³, and Amit Ranjan Trivedi¹

¹University of Illinois Chicago, Chicago, IL ²Capital One (work done at Intel) ³Intel
detto3@uic.edu, amitrt@uic.edu

arXiv:2509.15735v3 [cs.LG] 29 Sep 2025

Abstract—Large language models (LLMs) offer broad utility but remain prone to hallucination and out-of-distribution (OOD) errors. We propose *EigenTrack*, an interpretable real-time detector that uses the spectral geometry of hidden activations, a compact global signature of model dynamics. By streaming covariance-spectrum statistics such as entropy, eigenvalue gaps, and KL divergence from random baselines into a lightweight recurrent classifier, EigenTrack tracks temporal shifts in representation structure that signal hallucination and OOD drift before surface errors appear. Unlike black- and grey-box methods, it needs only a single forward pass without resampling. Unlike existing white-box detectors, it preserves temporal context, aggregates global signals, and offers interpretable accuracy-latency trade-offs.

Index Terms—Hallucination Detection, OOD Detection, Large Language Models, Spectral Analysis, Interpretability.

I. INTRODUCTION AND PRIOR WORKS

Large language/vision-language models (LLMs/VLMs) are increasingly applied in domains such as healthcare, law, and finance, but remain unreliable: they hallucinate and degrade sharply on out-of-distribution (OOD) inputs [1], [2]. Early detectors used surface signals like softmax confidence [3] or semantic-entropy surrogates [4], but ignored internal dynamics and failed under domain shift. More recent methods differ by access level: *black-box* approaches (SelfCheckGPT [5], CoNLI [6], Cost-Effective HD [7]) use ensembles or multiple generations, capturing context at the cost of latency; *grey-box* methods (DetectGPT [8], Fast-DetectGPT [9], Glimpse [10]) exploit log-probability curvature or partial logits, but remain snapshot-based; and *white-box* detectors probe hidden states but lack generality, e.g., MIND [11] streams activations without temporal context, LapEigvals [12] analyzes spectra per step, and ReDeEP [13] uses retrievals, while [14] tracks narrow shifts.

We argue that spectral signatures provide a principled basis for hallucination and OOD detection by compressing high-dimensional activations into compact descriptors of representation geometry. Eigenvalue distributions, entropy, and spectral gaps are sensitive to low-rank correlations and instabilities that emerge under distribution shift or hallucination. Unlike token-level probabilities, which capture only output-layer uncertainty, spectral statistics integrate across hidden layers and reveal global uncertainty dynamics. Moreover, spectral sig-

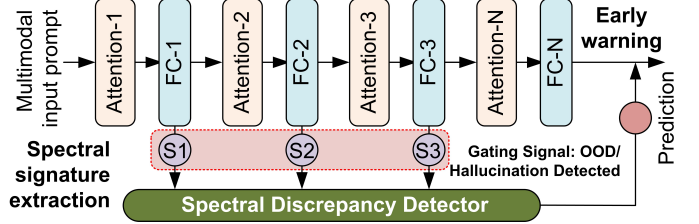


Figure 1. **EigenTrack**: Spectral signatures (such as entropy, spectral gap, divergence from random matrix baseline) are extracted from intermediate feed-forward layers and streamed into a recurrent spectral discrepancy detector. By tracking their temporal evolution, the detector generates early warnings of OOD or hallucination.

natures can also leverage fundamental laws from the random matrix theory such as the Marchenko–Pastur (MP) law [15], as shown in [16], which describes the eigenvalue distribution of isotropic noise; deviations from it provide a compact indicator of structure and thus hallucination or OOD onset.

Building on this insight, EigenTrack streams covariance spectra through a sliding window and feeds resulting statistics into a lightweight recurrent classifier (Fig. 1). Prior spectral methods such as RankFeat [17], SpectralGap [18], and SNoJoE [19] discriminate OOD from in-distribution via singular values or gaps, but operate on static snapshots and ignore temporal evolution. EigenTrack instead converts streaming spectral statistics into low-dimensional trajectories that expose how uncertainty builds over time.

Our contributions are: (i) a real-time detector, *EigenTrack*, that models temporal evolution of multi-layer spectral features to flag hallucination and OOD; (ii) an interpretable set of spectral indicators linking eigenvalue dynamics to latent representation shifts; and (iii) a data-generation pipeline for hallucination detection via multi-LLM interaction. EigenTrack achieves AUROC of 0.82–0.94 for hallucination and 0.85–0.96 for OOD, surpassing prior methods. On LLaMa-7B it reaches 0.89 for hallucinations and 0.92 for OOD, exceeding baselines such as HaloScope, LapEigvals, and SelfCheckGPT with only a lightweight recurrent head.

II. EIGENTRACK: METHODOLOGY

EigenTrack converts hidden activations of LLMs and VLMs into compact spectral descriptors and models their temporal evolution to detect hallucination and OOD behavior. The pipeline has three stages: (i) constructing a sliding-window

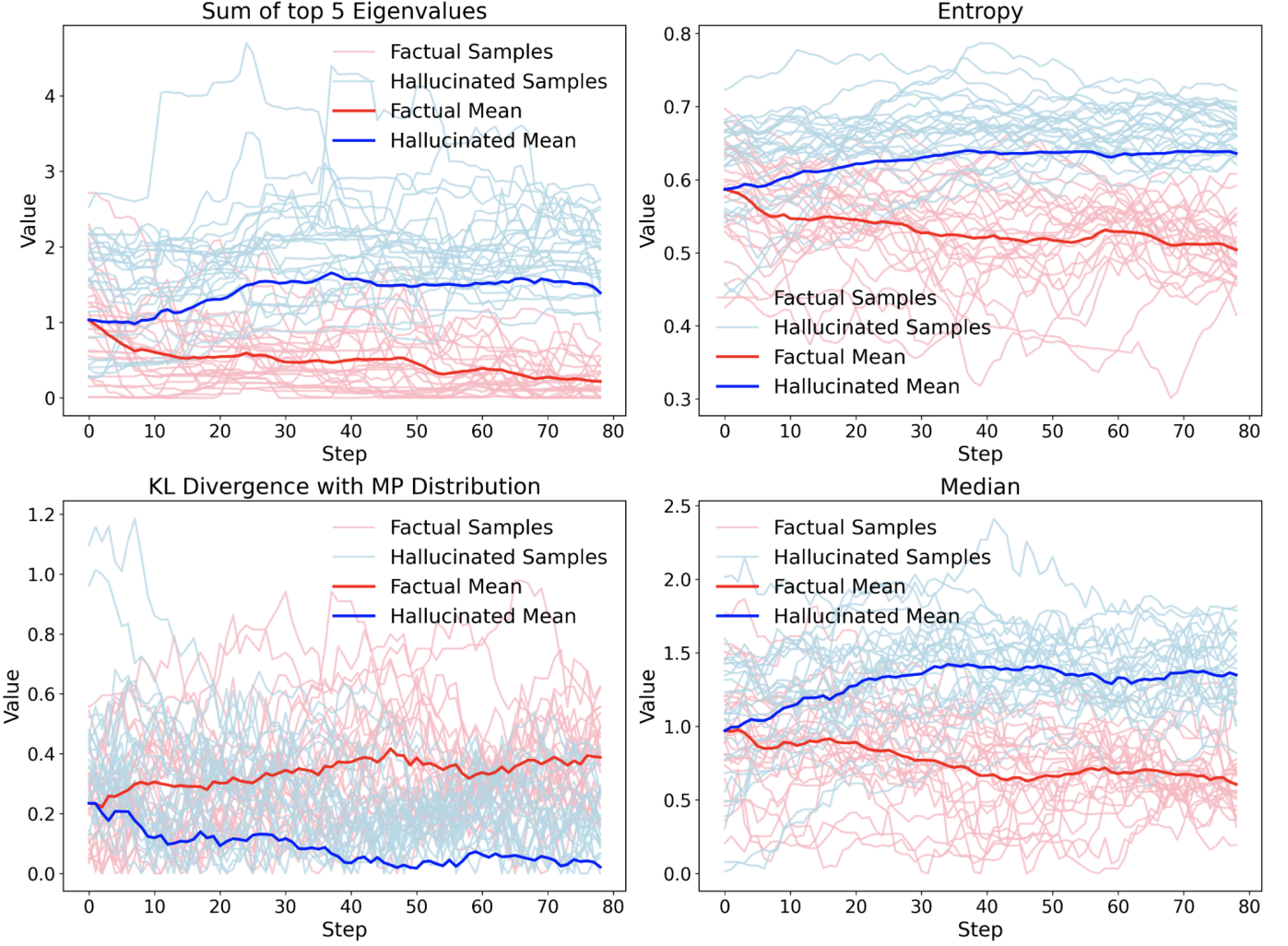


Figure 2. Evolution of spectral features over 80 steps on LLaMa-3B, comparing factual vs. hallucinated sequences, analyzed by the recurrent classifiers.

representation of activations, (ii) extracting spectral features that summarize the geometry and stability of the hidden state space, and (iii) classifying their temporal evolution with a lightweight recurrent model. This design rests on two principles: spectral statistics provide global, low-rank indicators of distributional shift, and temporal modeling enables cross-layer discrepancy identification for early detection before errors appear in the output.

Sliding-Window Representation: We select a set of m early transformer layers $L = \{\ell_1, \dots, \ell_m\}$, each producing activations $h_t^\ell \in \mathbb{R}^d$ at token t . Concatenating across layers yields $v_t = [h_t^{\ell_1} \parallel \dots \parallel h_t^{\ell_m}] \in \mathbb{R}^{md}$. Stacking the last N tokens forms a window matrix $H_t \in \mathbb{R}^{N \times md}$, updated at each step.

Spectral Feature Extraction: Instead of forming the covariance $C_t = \frac{1}{N} H_t^\top H_t$, we compute a truncated SVD $H_t = U_t \Sigma_t V_t^\top$ and recover eigenvalues $\lambda_{t,i} = \sigma_{t,i}^2 / N$. From these we build a k -dimensional feature vector F_t (default $k = 22$), including: (i) leading eigenvalues and cumulative variance, (ii) spectral gaps (e.g., $\lambda_{t,1} / \lambda_{t,2}$), (iii) entropy $S_t = -\sum_i p_{t,i} \log p_{t,i}$ with $p_{t,i} = \lambda_{t,i} / \sum_j \lambda_{t,j}$, and (iv) divergence from the Marčenko–Pastur reference law. These

capture signal instabilities, indicating hallucination or OOD.

Recurrent Classification: The feature sequence (F_1, \dots, F_T) is treated as a multivariate time series and processed by a lightweight recurrent model (RNN, GRU, or LSTM). At each step, F_t enters the recurrent cell, hidden states propagate context, and a feed-forward head outputs a binary logit for in-distribution vs. anomalous context. Weight sharing across time keeps the parameter count independent of sequence length, allowing the model to learn spectral signatures.

Hyperparameters and Extensions: EigenTrack supports tuning of the monitored layer set L , window length N , number of spectral features k , and recurrent hidden size to balance accuracy and latency. The pipeline also extends to multimodal architectures by constructing H_t from cross-modal fusion or vision encoder blocks.

III. RESULTS AND DISCUSSION

Experimental Setup: We evaluate EigenTrack on open-source HuggingFace LLMs (1B–8B parameters) from the LLaMa, Qwen, Mistral, and LLaVa families, covering both base and instruction-tuned variants. Each model generates up to 128 tokens. Hidden activations are streamed across layers.

Hallucination detection is tested on HaluEval (HotpotQA-based) by pairing each passage with its true question and a random question from LLaMa-8B, producing factual vs. hallucinated outputs. This forms an automatic data-generation pipeline involving three LLMs: a *Main Model* (the smallest one), a *Question Generator*, and an *Answer Judge*. These interact iteratively to yield labeled hallucinated and non-hallucinated responses from a QA-style dataset. For VLMs (e.g., LLaVa), passages are replaced with Flickr8k images.

OOD detection uses WebQuestions as in-distribution and Eurlex (legal-domain queries) as OOD, since such data is unseen in pretraining. For VLMs, we use the same questions paired with contextual images from Flickr8k. Again, an *Answer Judge* is employed to provide the final correctness judgment. EigenTrack converts activations into spectral feature sequences processed by recurrent classifiers (RNN, GRU, LSTM). Each classifier consists of a linear input layer, one recurrent layer, and a binary output head. Detection performance is reported using AUROC curve. AUROC values range from 0.5 (chance) to 1.0 (perfect discrimination).

Spectral Dynamics: Fig. 2 shows the temporal evolution of spectral features for factual and hallucinated sequences. Distinct and consistent patterns emerge. Hallucinations concentrate variance in a few dominant directions, reflected in higher sums of the top eigenvalues (top-left). Their spectra are flatter and more dispersed, leading to elevated entropy values (top-right). From a random matrix theory perspective, if activations were uncorrelated noise their eigenvalue distribution would follow the Marčenko–Pastur law [15]. Relative to this baseline, hallucinated sequences remain closer to the noise-like regime, yielding lower KL divergence (bottom-left), while factual sequences diverge more strongly, consistent with structured and informative dynamics. The median eigenvalue is also higher and more stable for hallucinations, whereas factual outputs show lower and more variable medians that track model confidence (bottom-right). *Overall*, hallucinations exhibit concentrated variance, flatter spectra, and noise-like behavior, i.e., spectral signatures reveal well before errors appear in the output.

Feature Contribution Analysis: A key question is *which spectral statistics are most critical for detection performance?* To examine this, we trained GRU classifiers on all triplets of spectral features (Table I). Results show that discriminative power is concentrated in a compact subset rather than spread uniformly across the feature space. In particular, measures of spectral power (mean or sum), leading eigenvalues, KL divergence from the Marčenko–Pastur baseline, and intermediate spectral gaps consistently appear in the most informative combinations, yielding AUROC values up to 0.79 for LLaMa-7B. Excluding these reduces performance to 0.69. Thus, a small set of interpretable descriptors is sufficient to capture shifts in activation geometry.

To validate this further, we applied SHAP (SHapley Additive exPlanations) to trained recurrent classifiers. SHAP assigns contribution values to each feature, allowing us to quantify which spectral statistics most strongly drive the recurrent classifier’s decision. Fig. 3 reports the five most influential

features per architecture. GRUs emphasize KL divergence, leading eigenvalue gaps, and entropy, i.e., the statistics that are tightly linked to structural instabilities, while LSTMs focus more on top- k eigenvalues, entropy, and KL divergence, reflecting their ability to model gradual drifts. Standard RNNs assign weight to central tendency measures (mean, median) alongside entropy and maximum eigenvalue, consistent with their simpler memory mechanisms. The figure further shows that GRUs concentrate nearly 80% of their attribution on the top ten features, whereas RNNs distribute importance more evenly.

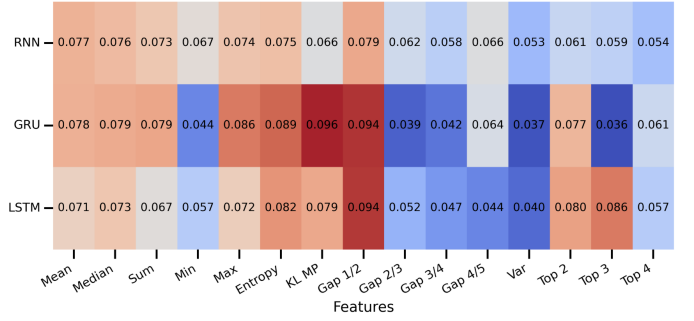


Figure 3. Heatmap (red: high, blue: low) showing the most important features for each recurrent classifier on LLaMa 3B, computed by SHAP. Spectral features such as spectral gap and entropy show higher SHAP value across classifiers.

Hallucination Detection: Table I shows that EigenTrack achieves robust hallucination detection, with AUROC between 0.82 and 0.94 across all tested LLMs. GRUs consistently deliver the best performance, followed by LSTMs and RNNs, highlighting the benefit of gated memory for tracking spectral dynamics. Performance scales with model size: moving from LLaMa-1B to LLaMa-7B adds about +0.05 AUROC, with the strongest results on 7B models (Qwen-7B and LLaVa-7B both exceeding 0.93 with GRU). Larger models appear to produce sharper, more stable spectral signatures that GRUs exploit more effectively than simpler recurrent cells. Compared to prior detectors on HaluEval, EigenTrack shows a clear margin: on LLaMa-7B it reaches 0.89 AUROC with GRU, surpassing HaloScope (0.86), LapEigvals (0.87), INSIDE (0.81), and even SelfCheckGPT on the larger LLaMa-30B (0.84). Similar gains hold across other models and methods (Table II).

OOD Detection: Table I shows a similar trend for OOD detection, with AUROC ranging from 0.85 to 0.96 and outperforming many state-of-the-art methods (Table II). GRUs again lead, with their advantage over other recurrent models most pronounced on smaller LLMs, indicating that gated memory is especially valuable when spectral signals are weaker. OOD detection often exceeds hallucination detection, suggesting that domain shifts induce more distinct spectral deviations than factual drift. By combining spectral features with temporal modeling, EigenTrack achieves state-of-the-art results on both hallucination and OOD detection, while requiring only a lightweight GRU head.

Table II reports AUROC comparison of EigenTrack against representative state-of-the-art detectors on LLaMa models of different scales. Across both hallucination and OOD settings, EigenTrack consistently achieves the highest scores, driven by

Table I

COMPARISON OF HALLUCINATION AND OUT-OF-DISTRIBUTION (OOD) DETECTION ACROSS LLMs AND VLMs OF VARYING SIZES USING DIFFERENT RECURRENT CLASSIFIERS (RNN, GRU, LSTM). WE REPORT AUROC AND F1 SCORES OBTAINED WITH THE FULL SPECTRAL FEATURE SET, AS WELL AS AUROC VALUES FOR THE BEST AND WORST TRIPLETS OF SPECTRAL FEATURES IDENTIFIED THROUGH ABLATION.

Model	AUROC Full			F1 Full			AUROC Best			AUROC Worst			
	RNN	GRU	LSTM	RNN	GRU	LSTM	RNN	GRU	LSTM	RNN	GRU	LSTM	
Hallucination	LLaMa 1B	0.799	0.842	0.831	0.750	0.790	0.783	0.725	0.774	0.758	0.597	0.644	0.630
	LLaMa 3B	0.832	0.861	0.844	0.779	0.808	0.794	0.760	0.779	0.772	0.632	0.662	0.645
	LLaMa 7B	0.853	0.894	0.872	0.805	0.851	0.825	0.771	0.789	0.778	0.656	0.698	0.668
	Qwen 1.8B	0.724	0.824	0.821	0.672	0.798	0.774	0.657	0.780	0.750	0.525	0.649	0.622
	Qwen 7B	0.842	0.931	0.922	0.794	0.881	0.870	0.773	0.813	0.810	0.646	0.726	0.718
	Mistral 7B	0.864	0.888	0.871	0.812	0.839	0.819	0.791	0.817	0.799	0.662	0.687	0.675
	LLaVa 7B	0.902	0.941	0.934	0.853	0.892	0.887	0.813	0.828	0.815	0.699	0.740	0.735
OOD	LLaMa 1B	0.825	0.855	0.852	0.776	0.814	0.802	0.753	0.793	0.781	0.626	0.666	0.652
	LLaMa 3B	0.858	0.892	0.871	0.810	0.841	0.821	0.787	0.788	0.779	0.660	0.693	0.671
	LLaMa 7B	0.879	0.924	0.897	0.829	0.874	0.847	0.801	0.807	0.805	0.680	0.724	0.692
	Qwen 1.8B	0.762	0.872	0.846	0.713	0.821	0.796	0.690	0.800	0.775	0.563	0.673	0.647
	Qwen 7B	0.867	0.948	0.936	0.817	0.898	0.885	0.796	0.815	0.814	0.669	0.747	0.736
	Mistral 7B	0.883	0.906	0.892	0.832	0.855	0.842	0.788	0.791	0.790	0.683	0.707	0.692
	LLaVa 7B	0.923	0.958	0.946	0.873	0.906	0.897	0.822	0.826	0.814	0.724	0.757	0.746

Table II
AUROC COMPARISON ON LLaMA FAMILY MODELS (1B/3B/7B)
BETWEEN EIGENTRACK AND OTHER SOTA METHODS.

Method	LLaMa-1B	LLaMa-3B	LLaMa-7B	
Hallucination	EigenTrack	84.2	86.1	89.4
	LapEigvals	78.5	81.9	87.1
	INSIDE	75.3	83.1	81.0
	SelfCheckGPT	73.9	80.4	80.9
	HaloScope	82.0	82.7	86.1
OOD	EigenTrack	85.5	89.2	92.4
	Cosine Distance	81.9	87.7	92.0
	Energy Score	83.2	85.2	89.0
	Max Softmax Prob	70.1	71.0	72.0
	ODIN	80.1	84.2	92.1

its use of temporal spectral statistics of hidden activations. These capture global representation dynamics that surface-level confidence methods (Max Softmax, ODIN) and snapshot spectral analyses (LapEigvals) miss. Baseline OOD methods are score-based without OOD supervision; their AUROC values are obtained by sweeping thresholds over in-distribution scores, ensuring threshold-independent and fair comparison.

Accuracy–Latency Trade-off: Fig. 4a shows AUROC and inference time as functions of sliding-window size for GRU classifiers on hallucination data. Shorter windows capture finer dynamics and raise AUROC but also increase latency, since more windows must be processed per sequence. Performance stabilizes between 25–50 tokens, offering a strong operating point across LLMs. Fig. 4b shows AUROC versus number of generated tokens: models begin near chance but gain accuracy rapidly in the first few tokens before plateauing. This indicates that hallucination cues emerge early, so practitioners can balance computation against accuracy by tuning window size or response length to prioritize either low latency or precision.

Why Spectral Signatures Work? Modern decoder-only LLMs apply LayerNorm at every transformer block [20], centering activations and scaling them to unit variance. Along with the near-orthogonality of projection matrices from weight

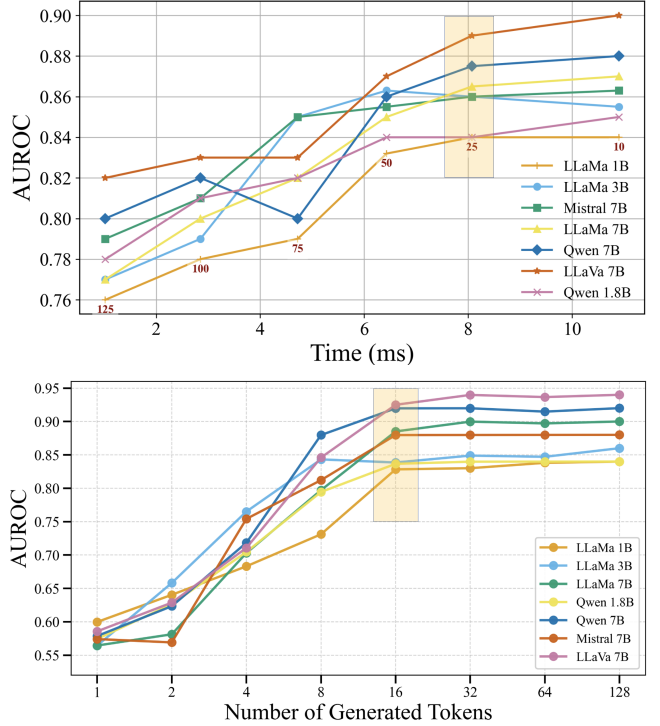


Figure 4. Performance trade-offs in EigenTrack: (a, top) AUROC–latency trade-off for different sliding-window lengths using GRU for hallucination detection; (b, bottom) AUROC at different stages of response generation, showing that later tokens yield more reliable predictions.

decay and Adam optimization [21], this makes per-token activations approximately mean-zero and isotropic. Under these conditions, the eigenvalue distribution of a sliding-window activation matrix $H_t \in \mathbb{R}^{N \times d}$ converges to the Marchenko–Pastur law, which serves as a principled *null baseline* for spectral statistics such as eigenvalue gaps [22]. Departures from this baseline align with our findings: OOD inputs or hallucinations perturb activations so hidden states follow a spiked covariance model, where correlations exceeding the Baik–Ben Arous–Péché threshold [23] cause eigenvalues to detach from the MP bulk. In practice, this yields

larger leading eigenvalues, reduced entropy, and widened gaps (Fig. 2), together with concentrated predictive power in KL divergence and eigenvalue-based statistics highlighted by ablation and SHAP analyses (Table I, Fig. 3). These deviations are mathematically well characterized and yield compact, low-dimensional signatures of instability.

IV. CONCLUSION

We introduced EigenTrack, a real-time and interpretable framework for detecting hallucinations and out-of-distribution behavior in LLMs and VLMs by modeling the temporal evolution of spectral features. Unlike output-layer heuristics, it uses eigenvalue-based descriptors and recurrent modeling to capture representation dynamics and enable early detection. Experiments show state-of-the-art performance across LLM and VLM families while remaining lightweight, tunable, and architecture-agnostic. Grounded in low-rank spectral statistics, EigenTrack provides a robust and generalizable basis for safety tools, with potential extensions toward adaptive generation and causal diagnostics.

ACKNOWLEDGMENT

This work was supported in part by a Gift funding from Intel, by CogniSense, one of the seven SRC/DARPA JUMP2.0 Centers, NSF CAREER Award # 2046435. The authors would also like to thank Nilesh Ahuja from Intel for valuable discussions.

REFERENCES

- [1] S. Tayebati, N. Darabi, D. Kumar, D. K. K. Dona, T. Tulabandhula, R. Krishnan, and A. R. Trivedi, “Cap: Conformalized abstention policies for context-adaptive risk management for llms and vlms,” in *Proceedings of the Asian Conference on Machine Learning (ACML)*, 2025.
- [2] D. Jayasuriya, S. Tayebati, D. Ettori, R. Krishnan, and A. R. Trivedi, “Sparc: Subspace-aware prompt adaptation for robust continual learning in llms,” in *Proceedings of the 2025 International Joint Conference on Neural Networks*, 2025.
- [3] D. Hendrycks and K. Gimpel, “A baseline for detecting misclassified and out-of-distribution examples in neural networks,” in *International Conference on Learning Representations*, 2017.
- [4] S. Farquhar and Y. Gal, “Semantic entropy: Language models detect and explain their failures,” *Transactions on Machine Learning Research*, 2024, arXiv:2305.17409.
- [5] P. Manakul, A. Liusie, and M. J. F. Gales, “Selfcheckgpt: Zero-resource black-box hallucination detection for generative large language models,” in *Proceedings of EMNLP 2023*, 2023, pp. 9004–9017.
- [6] D. Lei, Y. Li, M. Hu, M. Wang, V. Yun, E. Ching, and E. Kamal, “Chain of natural language inference for reducing large language model ungrounded hallucinations,” *arXiv preprint arXiv:2310.03951*, 2023.
- [7] S. Valentin, J. Fu, G. Detommaso, S. Xu, G. Zappella, and B. Wang, “Cost-effective hallucination detection for llms,” *arXiv preprint arXiv:2407.21424*, 2024.
- [8] E. Mitchell, Y. Lee, A. Khazatsky, C. D. Manning, and C. Finn, “Detectgpt: Zero-shot machine-generated text detection using probability curvature,” in *Proceedings of ICML 2023*, 2023, pp. 24 950–24 962.
- [9] G. Bao, Y. Zhao, Z. Teng, L. Yang, and Y. Zhang, “Fast-detectgpt: Efficient zero-shot detection of machine-generated text via conditional probability curvature,” *arXiv preprint arXiv:2310.05130*, 2023.
- [10] G. Bao, Y. Zhao, J. He, and Y. Zhang, “Glimpse: Enabling white-box methods to use proprietary models for zero-shot llm-generated text detection,” in *Proceedings of ICLR 2025*, 2025.
- [11] W. Su, C. Wang, Q. Ai, Y. Hu, Z. Wu, Y. Zhou, and Y. Liu, “Unsupervised real-time hallucination detection based on the internal states of large language models,” in *Findings of the Association for Computational Linguistics: ACL 2024*, 2024, pp. 14 379–14 391.
- [12] J. Binkowski, D. Janiak, A. Sawczyn, B. Gabrys, and T. Kajdanowicz, “Hallucination detection in llms using spectral features of attention maps,” in *Proceedings of ICML 2025*, 2025.
- [13] Z. Sun, X. Zang, K. Zheng, Y. Song, J. Xu, X. Zhang, W. Yu, and H. Li, “Redeep: Detecting hallucination in retrieval-augmented generation via mechanistic interpretability,” in *Proceedings of ACL 2025*, 2025.
- [14] A. Sriramanan, S. Shen, T. Dao *et al.*, “Attentionscore: Faithfulness detection from attention patterns in llms,” in *Proceedings of ICML 2024*, 2024, arXiv:2311.09516.
- [15] V. A. Marčenko and L. A. Pastur, “Distribution of eigenvalues for some sets of random matrices,” *Mathematics of the USSR-Sbornik*, 1967.
- [16] D. Ettori, N. Darabi, S. Senthilkumar, and A. R. Trivedi, “Rmt-kd: Random matrix theoretic causal knowledge distillation,” *arXiv preprint arXiv:2509.15724*, 2025.
- [17] Y. Song, Y. Huang, C. Yang, Y. Shi, D. Wei, L. Sun, and L. Chen, “Rankfeat: Rank-1 feature removal for out-of-distribution detection,” in *Advances in Neural Information Processing Systems (NeurIPS)*, 2022. [Online]. Available: https://proceedings.neurips.cc/paper_files/paper/2022/file/71c9eb0913e6c7fd3afed69c914b1a0c-Paper-Conference.pdf
- [18] J. Gu, Y. Qiao, and P. Li, “Spectralgap: Graph-level out-of-distribution detection via laplacian eigenvalue gaps,” *arXiv preprint arXiv:2505.15177*, 2025. [Online]. Available: <https://arxiv.org/abs/2505.15177>
- [19] Y. Mei, Z. Li, Y. Li, and J. Zou, “Spectral normalized joint energy for multi-label out-of-distribution detection,” *arXiv preprint arXiv:2405.04759*, 2024. [Online]. Available: <https://arxiv.org/abs/2405.04759>
- [20] A. Radford, J. Wu, R. Child, D. Luan, D. Amodei, and I. Sutskever, “Language models are unsupervised multitask learners,” *OpenAI Blog*, vol. 1, no. 8, p. 9, 2019.
- [21] S. Kobayashi, Y. Akram, and J. von Oswald, “Weight decay induces low-rank attention layers,” *arXiv preprint arXiv:2410.23819*, 2024.
- [22] N. Darabi, D. Naik, S. Tayebati, D. Jayasuriya, R. Krishnan, and A. R. Trivedi, “Eigenshield: Causal subspace filtering via random matrix theory for adversarially robust vision-language models,” *arXiv preprint arXiv:2502.14976*, 2025.
- [23] J. Baik, G. Ben Arous, and S. Péché, “Phase transition of the largest eigenvalue for nonnull complex sample covariance matrices,” *Annals of Probability*, vol. 33, no. 5, pp. 1643–1697, 2005.